Large Reactional Osteogenesis in Maxillary Sinus Associated with Secondary Root Canal Infection Detected Using Cone-beam Computed Tomography

Carlos Estrela, DDS, MSc, PhD, Olavo César Lyra Porto, DDS, MSc,* Nádia Lago Costa, DDS, MSc, PhD,* Marcel da Silva Garrote, DDS, MSc,* Daniel Almeida Decurcio, DDS, MSc, PhD,* Mike R. Bueno, DDS, MSc, PhD,[†] and Brunno Santos de Freitas Silva, DDS, MSc, PhD**

Abstract

Inflammatory injuries in the maxillary sinus may originate from root canal infections and lead to bone resorption or regeneration. This report describes the radiographic findings of 4 asymptomatic clinical cases of large reactional osteogenesis in the maxillary sinus (MS) associated with secondary root canal infection detected using cone-beam computed tomographic (CBCT) imaging. Apical periodontitis, a consequence of root canal infection, may lead to a periosteal reaction in the MS and osteogenesis seen as a radiopaque structure on imaging scans. The use of a map-reading strategy for the longitudinal and sequential slices of CBCT images may contribute to the definition of diagnoses and treatment plans. Root canal infections may lead to reactional osteogenesis in the MS. High-resolution CBCT images may reveal changes that go unnoticed when using conventional imaging. Findings may help define initial diagnoses and therapeutic plans, but only histopathology provides a definitive diagnosis. Surgical enucleation of the periapical lesion is recommended if nonsurgical root canal treatment fails to control apical periodontitis. *(J Endod 2015;■:1–11)*

Key Words

Apical periodontitis, cone-beam computed tomographic imaging, maxillary sinus, radiopaque lesion, reactional osteogenesis, root canal infection

From the *Department of Stomatology Sciences, Federal University of Goiás, Goiânia, Goiás; and [†]Department of Oral Sciences, University of Cuiabá, Cuiabá, Mato Grosso, Brazil.

Address requests for reprints to Prof Carlos Estrela, Department of Stomatology Sciences, Federal University of Goiás, Praça Universitária s/n, Setor Universitário, CEP: 74605-220, Goiânia, GO, Brazil. E-mail address: estrela3@terra.com.br

0099-2399/$ - see front matter

http://dx.doi.org/10.1016/j.joen.2015.09.004

The proximity of roots of the posterior maxillary teeth to the floor of the maxillary sinus (MS) favors the appearance of inflammation in this region (1–5). In some cases, these roots may project into the MS (5). On radiographs, the MS, the widest of the paranasal sinuses, is seen as a radiolucent oval structure outlined by a thin radiopaque line. MS shape, size, radiolucency, and wall thickness may vary depending on distinct radiographic projections in conventional imaging (6–9).

Root canal infection may affect the sinus mucosa even when there is no perforation of the cortical sinus floor, and infection may spread into the sinus (10–15), which explains a considerable number of MS abnormalities (16, 17). Odontogenic maxillary sinusitis has been associated with root canal infection (1–4, 6, 10–15). Shanbhag et al (4) evaluated the association between teeth with periapical lesions or periodontal disease and sinus mucosal thickening using cone-beam computed tomographic (CBCT) imaging. Scans of 485 sinuses (243 patients) were evaluated for the presence of periapical lesions or periodontal disease in the posterior maxillary teeth associated with mucosal thickening, which was classified as pathological when greater than 2 mm. Their results showed that mucosal thickening in the sinuses was highly prevalent (60.5%) and 9.75 times more likely to be associated with teeth with periapical lesions than with those without it. Bornstein et al (10) measured the thickness and evaluated the anatomic characteristics of the Schneiderian membrane and cortical bone using limited CBCT scans used to plan apical surgery of maxillary molars. The Schneiderian membrane near roots with apical lesions tended to be significantly thicker than in those without evident apical pathoses.

The promising advances of CBCT imaging and the detailed management of images of MS inflammation, which can be navigated in different planes, may provide a better understanding of cases, an accurate diagnosis, and, consequently, a better treatment plan (1–4, 10, 14, 15, 17–19).

Periapical radiopacities that reveal bone reaction are less common than periapical radiolucencies (20–22). Radiolucent areas are not often replaced with sclerotic bone after endodontic treatment, which may lead to misdiagnoses (9, 22, 23). This study describes 4 unusual clinical cases of large reactional osteogenesis in the MS associated with secondary root canal infection detected using CBCT imaging. In clinical cases with complex or nonspecific signs and symptoms, CBCT scans were obtained to define the diagnosis of periapical disease (24). In all cases, the referral to the private radiologic center was made only after a thorough clinical examination, appropriate diagnostic testing, and an explanation to the patient about why the referral was necessary.

Case Reports

Case 1

A 53-year-old woman was referred to a private radiologic center (CIRO, Goiania, GO, Brazil) for panoramic radiographs to investigate the cause of sporadic discomfort in teeth #2, #3, and #30 during mastication. Her medical history was negative for concomitant diseases. Clinical examination revealed root canal treatments and

Figure 1. (*A*) Radiograph shows singular appearance of root canal filling extending to the root apex and discreet apical radiolucency in the area of teeth #3, #4, and (*B*) #30. (*C*) Panoramic radiograph shows irregular opacity in the right MS. (*D* and *E*) CBCT scan shows a hypodense periapical lesion with a small amount of irregular mixed content and irregular bone extension into the right MS.

restorations in these teeth and did not show any abnormalities of the periodontal tissues. There was no spontaneous symptom or edema, and mobility was normal. Palpation of buccal and lingual structures around these teeth did not reveal any clinical evidence of endodontic disease. Radiographs showed a root canal filling extending to the root apex and discreet apical radiolucencies in teeth #3, #4, and #30. Tooth #3 had a well-adapted endodontic post with its volume centered in the root canal (Fig. 1*A* and *B*). Tooth #31 responded positively to cold testing. Panoramic images showed an irregular radiopaque structure in the right MS (Fig. 1*C*). To investigate patient discomfort, CBCT scans were obtained using the I-CAT Cone Beam 3D imaging system (Imaging Sciences International, Hatfield, PA). Volumes were reconstructed using isotropic-isometric voxels measuring 0.20 × 0.20 × 0.20 mm. Scans of the teeth affected were obtained in sagittal, coronal, and axial planes. In the mesiobuccal root of tooth #3, the CBCT images showed an area of bone hypodensity involving the root apex with irregular internal margins, some straight and some concave, which suggested the absence of growth under pressure. In addition, external limits were marked by cortical bone and sharp external angles (Fig. 1*D* and *E*). An irregular bone extension into the

Case 1

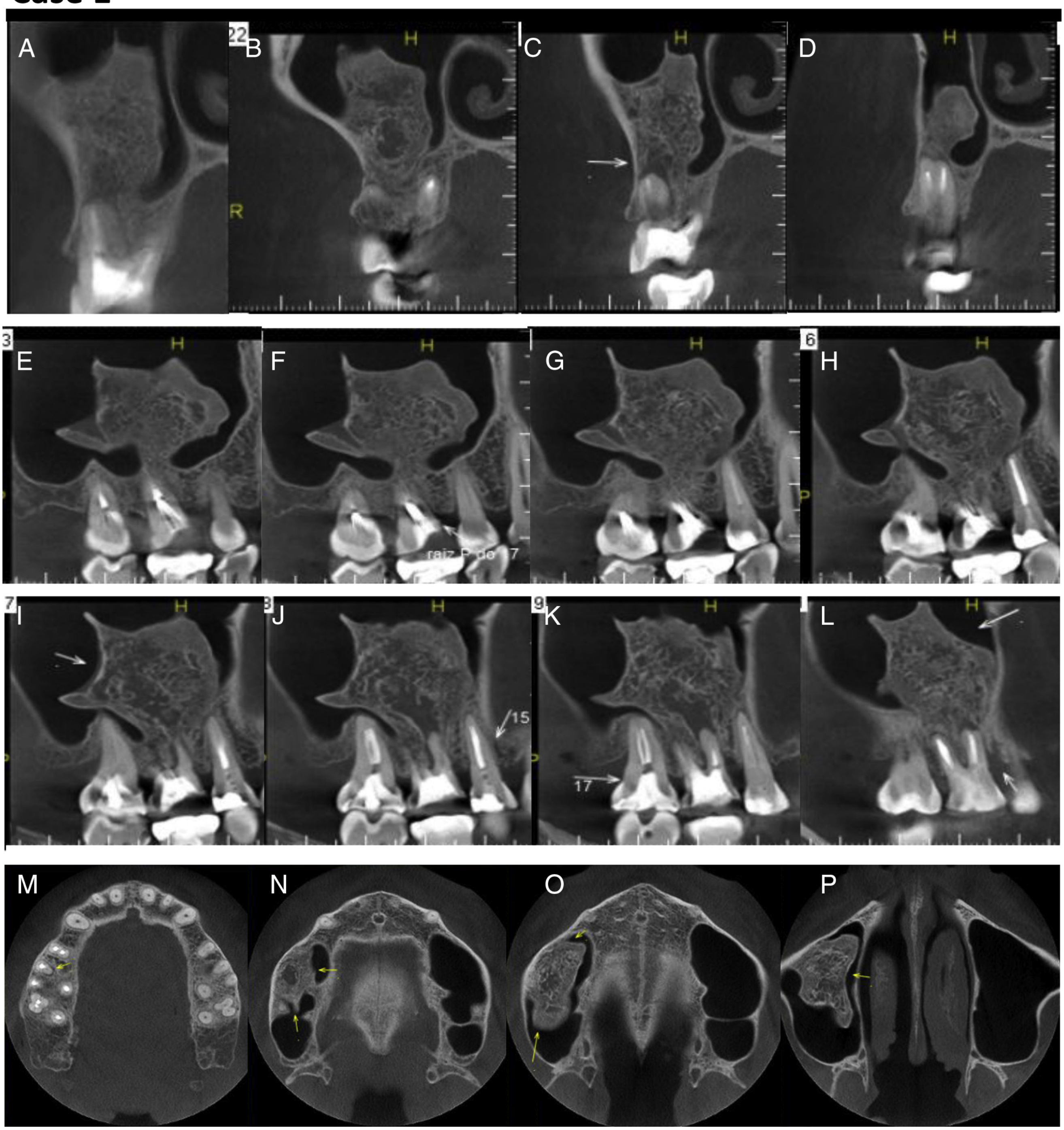

Figure 2. (*A*–*P*) CBCT scan shows a large area of apparent cancellous bone surrounded by a thin extension of cortical bone into the right MS.

right MS had a large area of what apparently was cancellous bone formation surrounded by a thin cortical layer (Figs. 1*D* and *E* and 2*A–P*). The treatment suggested was the surgical removal of the tissue and the root apex that had apical periodontitis.

The surgical procedures to remove the bone lesion in the right MS began with antibacterial conditioning of the oral cavity followed by general anesthesia after nasotracheal intubation. The Caldwell-Luc approach was used as follows: intraoral incision, periosteal detachment, careful osteotomy of the tissue to preserve the integrity of the MS wall, detection and removal of the lesion, root end resection (apicoectomy) with removal of 3 mm of the apical end of the mesiobuccal root, irrigation and aspiration, review of the surgical cavity, and suture (Fig. 3*A–H*). Only apicoectomy was performed to avoid keeping the patient under general anesthesia in the operating room for a long surgical time and because of the satisfactory clinical quality of the root canal filling. All the material collected was sent for microscopic analysis.

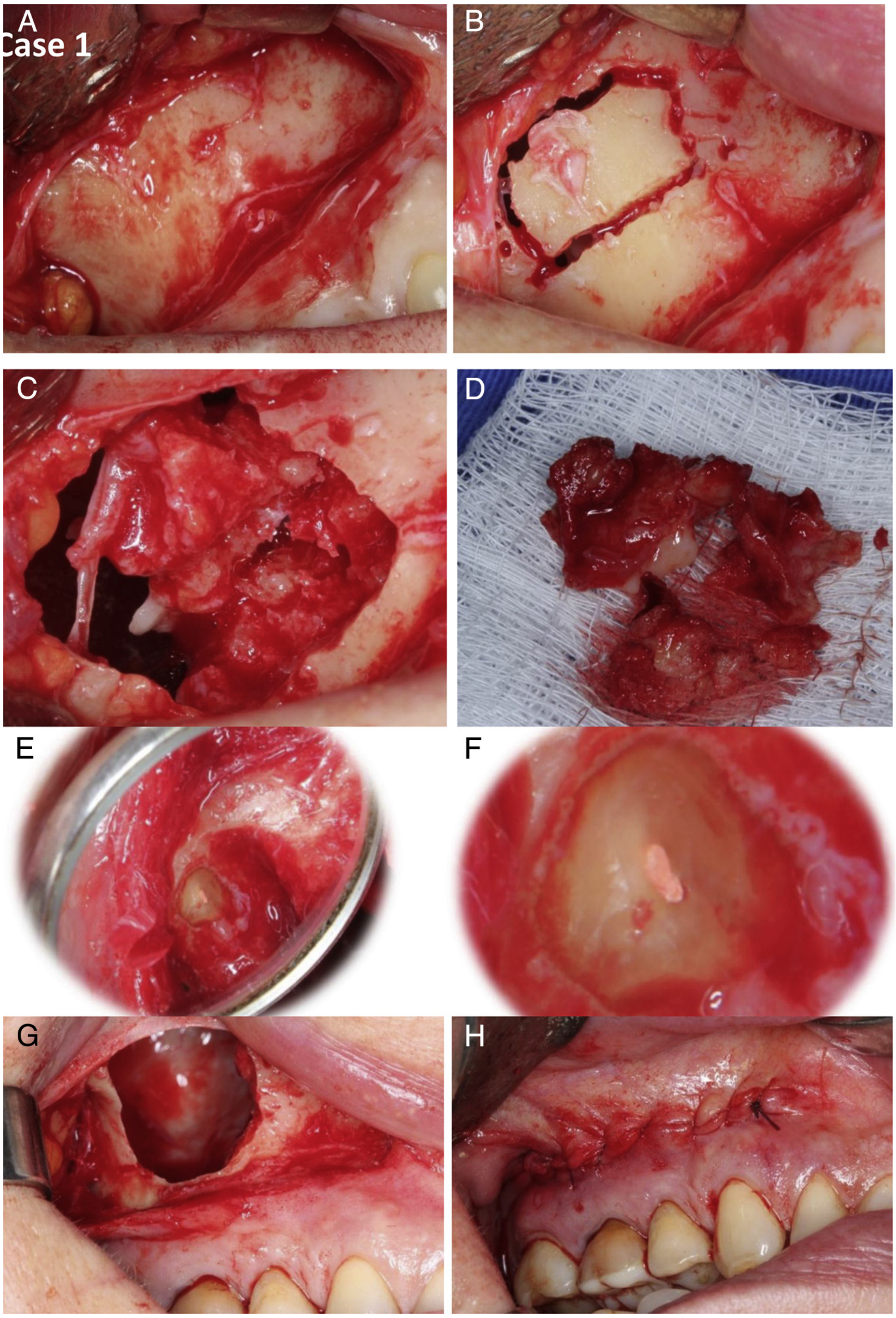

Figure 3. (*A* and *B*) Surgical enucleation of the lesion using the Caldwell-Luc approach. (*C* and *D*) Careful removal of the tissue to preserve the integrity of the MS wall. (*E* and *F*) Root end resection: removal of 3 mm of the apical root end of the mesiobuccal root (apicoectomy). (*G* and *H*) Irrigation and aspiration; a review of the surgical cavity and suture.

The patient returned 7 days later for clinical evaluation and suture removal. At the follow-up visit 2 weeks after surgery, the mucosal wound had healed completely. The patient did not complain of any clinical symptoms or discomfort during mastication. The importance of keeping the scheduled follow-up visits was reinforced.

The periapical lesion was examined macroscopically to describe its shape, color, and consistency. All specimens were fixed in 10% buffered formalin (pH = 7.4) and embedded in paraffin. The microscopic features were evaluated by the analysis of a 5-μm section of each sample stained routinely with hematoxylin-eosin. Histopathology revealed osteogenesis at distinct stages of maturation, mature bone tissue with concentric layers of lamellae (cement lines), and organized Harversian systems in the upper area of the specimen. MS mucosa, seen adjacent to bone, was a bilaminar membrane with ciliated columnar epithelial cells, similar to respiratory epithelium, and permeated by a small amount of chronic inflammatory infiltrate (Fig. 4*A*). There were also large trabeculae of mature lamellar bone and mature fibrofatty tissue and marrow (Fig. 4*B*). Adjacent to the apical region, immature bone had a large number of osteocytes and disorganized collagen fibers (Fig. 4*C*).

Case 2

A 41-year-old woman was referred to a private radiology center (Goiania, GO, Brazil) for imaging studies to plan the placement of maxillary implants. Her medical history was negative for concomitant disease. Clinical examination revealed the absence of anterior maxillary incisors and first and second molars that were replaced with dental prostheses. There were no spontaneous symptoms or edema, and both mobility of teeth #4, #5, and #6 and periodontal tissue attachment were normal. Palpation of buccal and lingual structures around this site revealed no abnormalities. The response to pulp vitality testing of teeth #1 and #4 was normal. The diagnosis was apical periodontitis of tooth #6. CBCT imaging was indicated, and images were acquired using the I-CAT Cone Beam 3D imaging system. CBCT scans showed areas of bone hypodensity in the root apex with irregular internal margins and a projection into the right MS, which suggested the absence of growth under pressure (Fig. 5*A–D*). A heterogeneous hyperdense oval structure with irregular mixed contents was noted in the area of tooth #6 (Fig. 5*B–D*). Adjacent to the maxillary area of osteogenesis, there was a mucous retention cyst in the right MS (Fig. 5*A* and *B*). Nonsurgical root canal retreatment of tooth #6 was recommended, and if apical periodontitis were not resolved, surgical enucleation of the periapical lesion would be indicated.

Case 3

A 68-year-old woman was referred to a private radiology center (Goiania, GO, Brazil) for imaging studies to plan the placement of an implant in the right posterior maxillary region. Her medical history was negative for concomitant diseases. Clinical examination revealed the presence of a full-coverage restoration in tooth #3 and no abnormalities of periodontal tissues. There was no spontaneous symptom or edema, and mobility was normal. Cold testing of tooth #4 was negative. Palpation of buccal and lingual structures around the tooth did not reveal any abnormalities. The diagnosis was apical periodontitis of tooth #3 and pulpal necrosis of tooth #4. CBCT imaging was indicated, and images were acquired using the I-CAT Cone Beam 3D imaging system. CBCT scans showed a well-defined hypodense periapical lesion associated with the apex of the lingual root of tooth #3. In addition, a cortical bone expansion into the right MS was associated with a heterogeneous

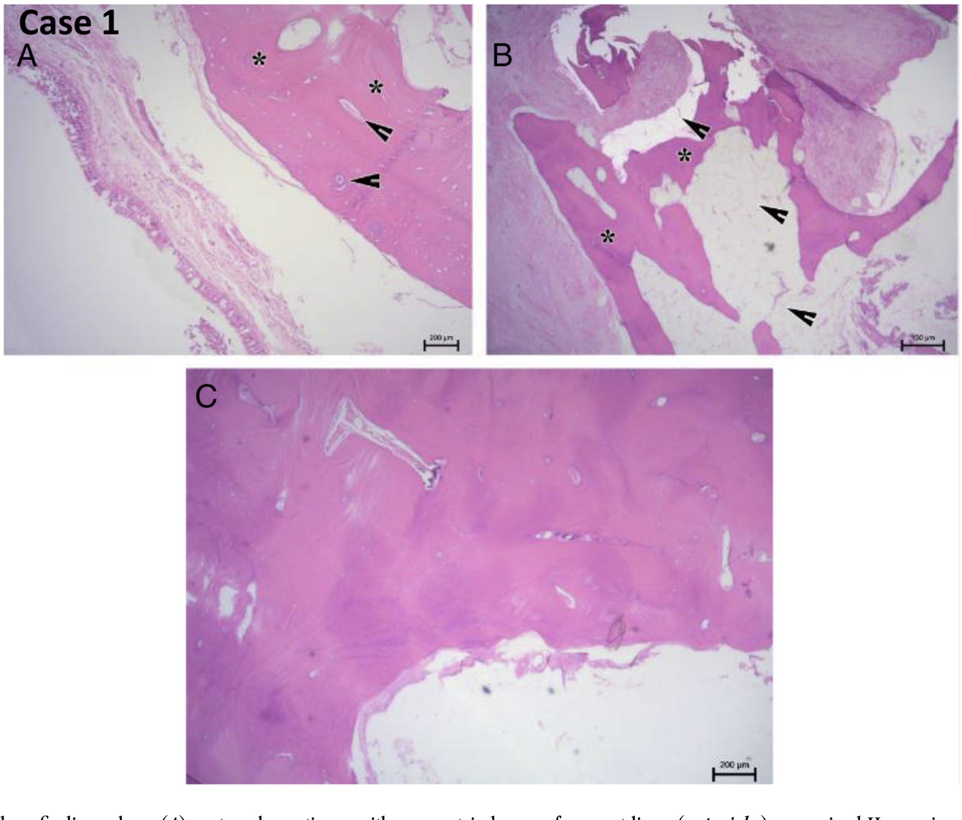

Figure 4. Histopathology findings show (*A*) mature bone tissue with concentric layers of cement lines (*asterisks*), organized Harversian systems, and maxillary sinus mucosa permeated by slightly chronic inflammatory infiltrate (*arrowheads*). (*B*) Large trabeculae of mature lamellar bone (*asterisks*) and mature marrow fibrofatty tissue (*arrowheads*). (*C*) Immature bone with a large number of osteocytes and disorganized collagen fibers (hematoxylin-eosin).

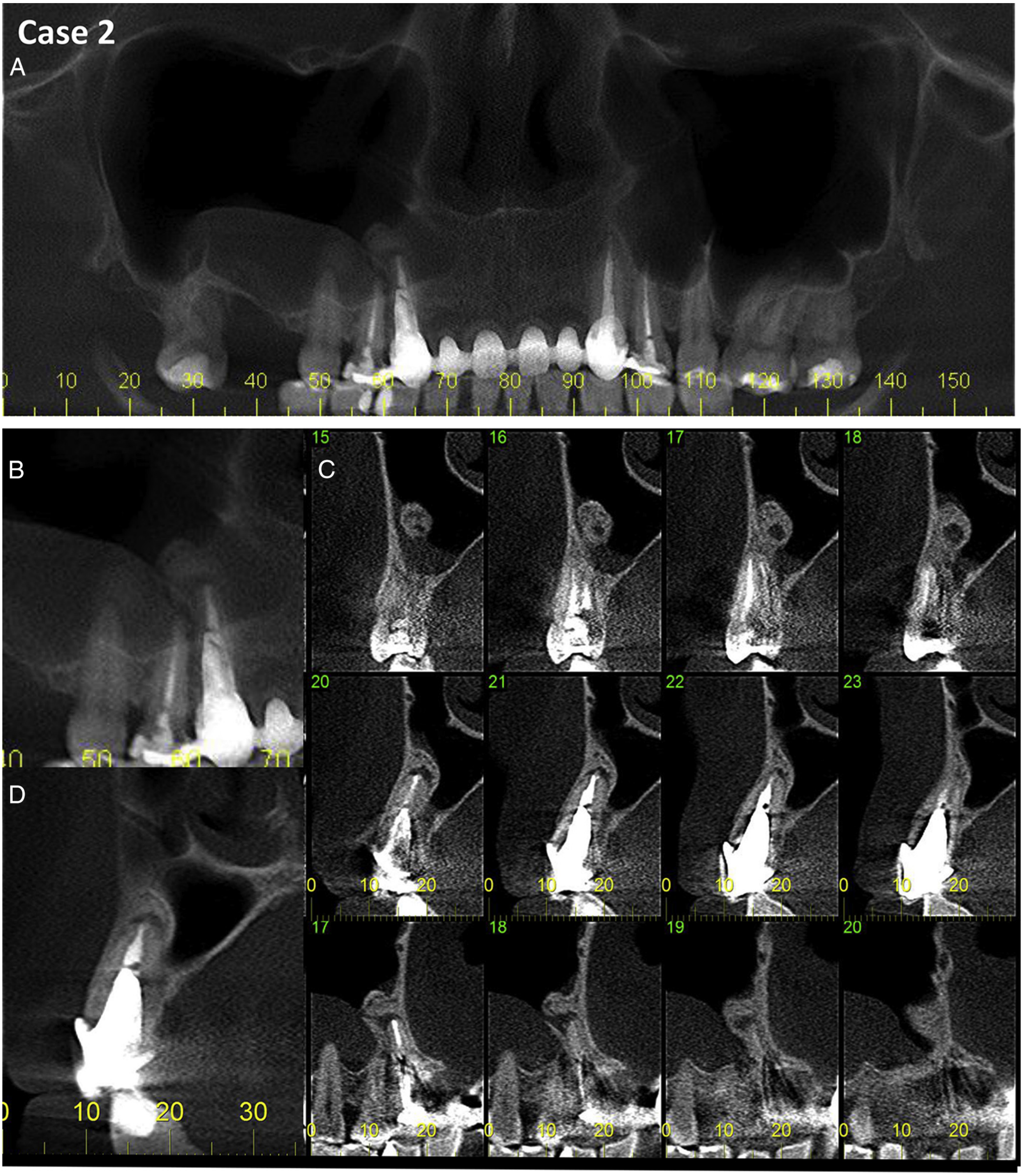

Figure 5. (*A–D*) CBCT scan of tooth #6 shows a circumscribed hypodense periapical lesion projecting into the right MS. (*B–D*) Heterogeneous hyperdense oval structure associated with tooth #6 contains irregular mixed contents. (*A* and *B*) Mucous retention cyst adjacent to maxillary bone formation in the right MS.

hyperdense oval structure near tooth #3. Findings suggested the absence of growth under pressure (Fig. 6*A–D*). Nonsurgical root canal treatment was indicated for tooth #4 and nonsurgical endodontic retreatment for tooth #3. If apical periodontitis was not resolved, surgical enucleation of the periapical lesion would be recommended.

Case 4

A 46-year-old woman was referred to a private radiology center (CROIF, Cuiabá, MT, Brazil) for imaging studies because of discomfort in the region of right maxillary teeth. Clinical examination revealed a sinus tract but no other tissue abnormalities. Medical history was negative

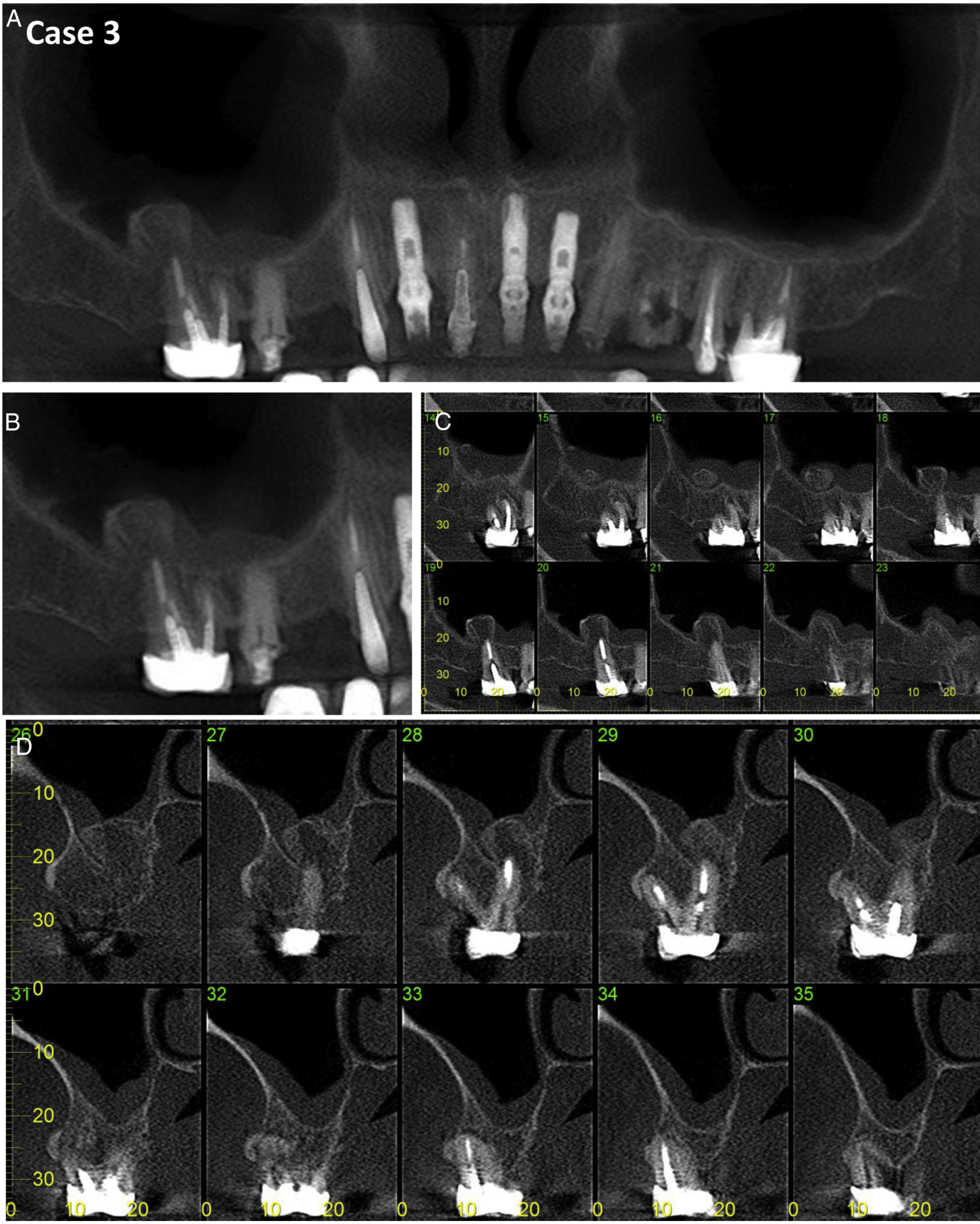

Figure 6. (*A*) A panoramic view shows well-defined hypodense periapical lesion associated with a heterogeneous hyperdense oval structure near tooth #3. (*B–D*) CBCT scan shows periapical lesion associated with lingual root of tooth #3 projecting into the MS.

for concomitant diseases. CBCT imaging was indicated, and images were acquired using the I-CAT Cone Beam 3D imaging system. Panoramic and periapical radiographs showed root canal treatment of teeth #3 and #4 and a dome-shaped thickening, similar to a mucous retention pseudocyst, in the right MS but with a thicker upper limit than usual. The right and left MS extended into the alveolar region. No periapical lesion was detected (Fig. 7*A* and *B*). CBCT scans (Fig. 8*A–C*) revealed that tooth #3 had a large periapical lesion surrounded by a thick layer of hyperdense bone that appeared to be an area of osteogenesis. The internal margins were irregular, some concave, which indicated the absence of growth under pressure. The diagnosis was apical periodontitis of tooth #3, and nonsurgical root canal retreatment was indicated to control infection followed by monitoring. If the lesion was not healed, surgical enucleation of the periapical lesion would be recommended.

Discussion

The radiopaque lesions described in this report were incidental findings. The imaging appearances of reactional osteogenesis in the MS were associated with secondary root canal infection in adult patients. The radiopaque lesions were asymptomatic, localized, and well-defined, and their shape was irregular, round, or ovoid. After the probable etiologic agents of osteogenesis had been detected, either root canal treatment or surgical enucleation was indicated.

The purpose of inflammatory responses is to detect, isolate, and destroy aggressive agents and ensure that the environment is favorable for repair (25). Resorption and bone regeneration are controlled by inflammatory mediators. Bone reactions depend on the intensity of the pathogenic agent as well as the duration of the aggression and the systemic health of the individual (23, 25). Inflammatory lesions in maxillary premolars and molars may induce periosteal reactions in the MS and lead to the formation of a bone layer called a halo effect (23).

Several studies have analyzed osteogenic responses caused by root canal infection (26, 27). The bone-resorbing activity of mature osteoclasts results from the interaction between membrane-bound RANK ligand (RANKL) and its receptor, receptor activator of nuclear factor kappa-B (RANK). RANKL-RANK signaling, which activates the nuclear factor-kB, is primarily inhibited by a soluble form called osteoprotegerin (OPG). Bone resorption promoted by the balance between RANKL and OPG is reciprocally regulated by interleukin (IL)-1, IL-6, IL-11, IL-17, macrophage colony-stimulating factor (M-CSF), granulocyte-macrophage colony-stimulating factor (GM-CSF), and tumor necrosis factor alpha. Th17 lymphocytes participate in osteoclastogenesis by recruiting polymorphonuclear cells, macrophages, and monocytes stimulated by the secretion of the master proinflammatory cytokine IL-17, GM-CSF, IL-1, IL-6, IL-8/CXCL8, and GROa/CXCL1 and the expression of RANKL (26). At the same time, other cytokines, such as interferon (IFN)-γ and IL-10, decrease the ratio of RANKL-OPG expression and attenuate bone resorption (26). A recent study found mesenchymal stem progenitor cells (STRO-1 and CD146) in inflamed periapical tissues and showed their great osteogenic potential, but their *in vivo* bone formation properties remain unclear (27). Márton and Kiss (26) critically discussed regulatory mechanisms that control the activity of host effector cells and signaling molecules during interactions with pathogenic microbes. Inflammatory reactions in the periapical tissues

Figure 7. (*A* and *B*) Panoramic and periapical radiographs show root canal treatment of teeth #3 and #4 and dome-shaped thickening similar to mucous retention pseudocyst in the right MS; the upper limit is thicker than usual. The right and left MS extend to the alveolar region; the images show no periapical lesions.

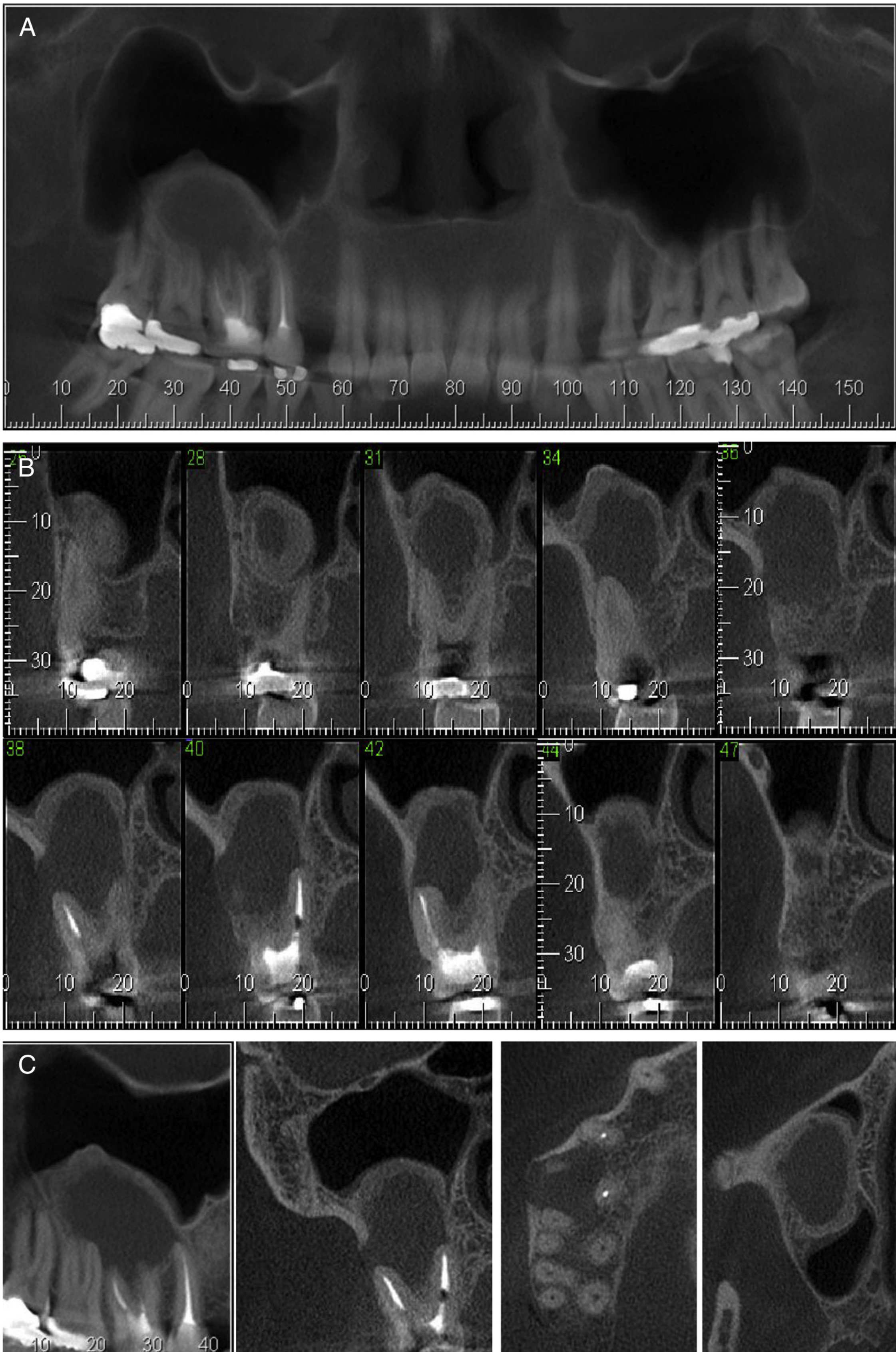

Figure 8. (*A–C*) CBCT scan shows root canal treatment of tooth #3 with a large periapical lesion surrounded by a thick layer of hyperdense bone that appears to be reactional osteogenesis; internal margins are irregular and some are concave, which suggests the absence of growth under pressure.

in response to endodontic infection are self-limiting in most cases. Both microbial influx from the infected root canal and excessive destruction of tooth-supporting structures are controlled for extended periods by complex interactions between immunoinflammatory cells and soluble mediators. The permanent shift between anti- and proinflammatory processes affects the balance between tissue destruction and regeneration at different stages of apical periodontitis. This dynamic balance between protection from infection and host tissue injury and repair is driven by overlapping networks of pleiotropic and redundant regulatory mechanisms.

The thin and uniform sinus mucosa (Schneiderian membrane) is composed of connective tissue through which the neurovascular bundles run, lining the inside of the MS. This membrane is firmly attached to the periosteum (10–15), which is composed of dense and fibrous collagenous connective tissue as well as osteoblasts and osteoclasts, young cells, undifferentiated cells, and even bone tissue stem cells. However, when an inflammatory response in the periosteum results from the low-intensity, prolonged action of aggressive agents that act directly or indirectly on its structure, the periosteum may react by producing new bone on the superficial cortical layers (23). Srouji et al (28) analyzed the osteogenic potential of the human maxillary sinus Schneiderian membrane (hMSSM) using both *in vitro* and *in vivo* assays. Samples of hMSSM were used to prepare cell cultures for histologic studies. Results showed that hMSSM cells could be induced to express alkaline phosphatase, bone morphogenic protein-2, osteopontin, osteonectin, and osteocalcin and to mineralize their extracellular matrix. Cells derived from explants of hMSSM grow in culture, express markers of osteoprogenitor cells, undergo osteogenic differentiation, and are transplanted *in vivo*; therefore, histologic evidence of osteogenesis may be found at the site of transplantation. The data accrued from this investigation show evidence of the presence of osteoprogenitor cells within the Schneiderian membrane.

In the first case described in this report, conventional images showed the root canal filling and a modest apical radiolucency in the regions of teeth #3, #4, and #30. Panoramic images showed an irregular opacity in the right MS; CBCT images showed a hypodense periapical lesion, a small amount of irregular mixed contents, and an irregular bone extension into the right MS (Figs. 1 and 2). The histopathological analysis revealed new bone at different stages of maturation. Adjacent to this bone, the MS mucosa was a bilaminar membrane with ciliated columnar epithelial cells that had the appearance of respiratory epithelium permeated by chronic inflammatory cells (Fig. 4*A*). Moreover, there were large trabeculae of mature lamellar bone and the mature fibrofatty tissue characteristic of the marrow (Fig. 4*B*). Adjacent to the apical region, immature bone had a large number of osteocytes and disorganized collagen fibers (Fig. 4*C*). These clinical, radiographic, and microscopic findings are evidence of the association between chronic periapical reaction and MS floor periostitis that stimulates bone reactions in particular ways. The same type of reactional osteogenesis was found in cases 2, 3, and 4 in which it was also associated with secondary root canal infections. From a clinical point of view, treatment in all cases should eliminate the infection responsible for the inflammation that stimulated bone reaction. The lesion was enucleated only in the first case.

Because this condition is often asymptomatic, most cases are detected incidentally in imaging studies. Araki et al (29) reported that, although the cause of most radiopaque lesions in the jaws is unclear, the etiologic factors for some of these lesions are gradually being discovered. Most radiopaque lesions are asymptomatic and are discovered incidentally on panoramic scans or CBCT images obtained during preoperative assessment for the placement of dental implants.

The normal sinus mucosa is not visualized on conventional radiographs; a negligible mucosal thickening may be seen as a normal radiographic finding (4), but mucosal thickening greater than 2 mm may suggest maxillary sinusitis (2, 12). Periapical radiolucencies are not clearly detected on periapical radiographs (18, 19). This study found radiopacities that extended into the MS, confirming the valuable contribution of CBCT imaging in the detection of radiopacities associated with infection of the root canal in the MS. The importance of the use of this imaging modality lies in the fact that it not only facilitates diagnostic imaging but may also help define alternatives to surgical enucleation, particularly when the removal of the lesion affects the MS walls.

Clinicians detect periapical radiolucencies more often than periapical radiopacities during the diagnosis of a periapical lesion and the planning of its treatment (20, 21, 29). Specific features of radiopaque periapical lesions were found in this report as well as changes associated with the site of their development. The differential diagnosis, based on clinical history, conventional radiographs, and histopathological analysis, should include osteitis, sclerosing osteitis, periapical cement dysplasia, sclerotic bone, and osteomyelitis with proliferative periostitis. In the current case reports, the periapical changes suggested a periapical reactional osteogenesis secondary to infection of root canal.

In summary, asymptomatic radiopaque periapical lesions are often incidental findings, and reactional osteogenesis in the MS is promoted by root canal infection. The detailed management of high-resolution CBCT images, which may reveal changes that go unnoticed when using conventional imaging modalities, may help define an initial diagnostic hypothesis and the treatment plan. The definitive diagnosis for some periapical lesions will only be made by histopathological findings. Nonsurgical root canal treatment should be indicated, and if it does not resolve apical periodontitis, surgical enucleation of the periapical lesion should be recommended.

Acknowledgments

The authors deny any conflicts of interest related to this study.

References

1. Nurbakhsh B, Friedman S, Kulkarni GV, et al. Resolution of maxillary sinus mucositis after endodontic treatment of maxillary teeth with apical periodontitis: a cone-beam computed tomography pilot study. J Endod 2011;37:1504–11.
2. Lu Y, Liu Z, Zhang L, et al. Associations between maxillary sinus mucosal thickening and apical periodontitis using cone-beam computed tomography scanning: a retrospective study. J Endod 2012;38:1069–74.
3. Pagin O, Centurion BS, Rubira-Bullen IRF, Capelozza ALA. Maxillary sinus and posterior teeth: accessing close relationship by cone-beam computed tomographic scanning in a Brazilian population. J Endod 2013;39:748–51.
4. Shanbhag S, Karnik P, Shirke P, Shanbhag V. Association between periapical lesion and maxillary sinus mucosal thickening: a retrospective cone-beam computed tomographic study. J Endod 2013;39:853–7.
5. Shankar L, Evans K, Hawke M, et al. *An Atlas of Imaging of the Paranasal Sinuses*. London: Martin Dunitz; 1994.
6. Allard RHB, van der Kwast WAM, van der Waal I. Mucosal antral cysts. Review of the literature and report of a radiographic survey. Oral Surg Oral Med Oral Pathol 1981;51:2–9.
7. Jensen OT. *The Sinus Bone Graft*. Carol Stream, IL: Quintessence Publishing Co; 1999:201–8.
8. Gnepp DR. *Diagnostic Surgical Pathology of the Head and Neck*. Philadelphia: WB Saunders; 2001.
9. Neville BW, Damm DD, Allen CM, Bouquot JE. *Oral and Maxillofacial Pathology*. Philadelphia: WB Saunders Company; 1995:119–52.
10. Bornstein MM, Wasmer J, Sendi P, et al. Characteristics and dimensions of the Schneiderian membrane and apical bone in maxillary molars referred for apical surgery: a comparative radiographic analysis using limited cone beam computed tomography. J Endod 2012;38:51–7.

11. Haumman CHJ, Chandler NP, Tong DC. Endodontic implications of the maxillary sinus: a review. Int Endod J 2002;35:127–41.
12. Rak KM, Newell JD, Yakes WF, et al. Paranasal sinuses on MR images of the brain: significance of mucosal thickening. AJR Am J Roentgenol 1991;156:381–4.
13. Gosau M, Rink D, Driemel O, Draenert FG. Maxillary sinus anatomy: a cadaveric study with clinical implications. Anat Rec 2009;292:352–4.
14. Maillet M, Bowles WR, McClanahan SL, et al. Cone-beam computed tomography evaluation of maxillary sinusitis. J Endod 2011;37:753–7.
15. Nair UP, Nair MK. Maxillary sinusitis of odontogenic origin: cone-beam volumetric computerized tomography-aided diagnosis. Oral Sur Oral Med Oral Pathol Oral Radiol Endod 2010;110:e53–7.
16. Havas TE, Motbey JA, Gullane PJ. Prevalence of incidental abnormalities on computed tomographic scans of the paranasal sinuses. Arch Otolaryngol Head Neck Surg 1988;114:856–9.
17. Rege ICC, Sousa TO, Leles CR, Mendonça EF. Occurrence of maxillary sinus abnormalities detected by cone beam CT in asymptomatic patients. BMC Oral Health 2012;12:30.
18. Cotton TP, Geisler TM, Holden DT, et al. Endodontic applications of cone beam volumetric tomography. J Endod 2007;33:1121–32.
19. Estrela C, Bueno MR, Leles CR, et al. Accuracy of cone beam computed tomography and panoramic and periapical radiography for detection of apical periodontitis. J Endod 2008;34:273–9.
20. Bender IB, Mori K. The radiopaque lesion: a diagnostic consideration. Endod Dent Traumatol 1985;1:2–12.
21. Monahan R. Periradicular and localized radiopacities. Dent Clin North Am 1994;38:113–6.
22. Kosti E, Lambrianidis T, Chatzisavvas P, Molyvdas I. Healing of a radiolucent periradicular lesion with periradicular radiopacity. J Endod 2004;30:548–50.
23. Lee L. Maxillary inflammatory lesions. In: White SC, Pharoah MJ, eds. *Oral Radiology–Principles and Interpretation,* 5th ed. St Louis: Mosby; 2007:363–78.
24. American Association of Endodontics, American Academy of Oral and Maxillofacial Radiology. Use of cone-beam computed tomography in endodontics. Joint Position Statement. Oral Surg Oral Med Oral Pathol Oral Radiol Endod 2011;111:234–7.
25. Consolaro A, Consolaro RB. The bone reactional capability and the names of inflammatory bone diseases. Dent Press Implantol 2012;6:18–25.
26. Márton IJ, Kiss C. Overlapping protective and destructive regulatory pathways in apical periodontitis. J Endod 2014;40:155–63.
27. Liao J, Shahrini MA, Al-Habibi M, et al. Cells isolated from inflamed periapical tissue express mesenchymal stem cell markers and are highly osteogenic. J Endod 2011;37:1217–24.
28. Srouji S, Kizhner T, Ben David D, et al. The Schneiderian membrane contains osteoprogenitor cells: *in vivo* and *in vitro* study. Calcif Tissue Int 2009;84:138–45.
29. Araki M, Matsumoto N, Matsumoto K, et al. Asymptomatic radiopaque lesions of the jaws: a radiographic study using cone-beam computed tomography. J Oral Sci 2011;53:439–44.